JOURNAL OF NANO- AND ELECTRONIC PHYSICS
Vol. **6** No 1, 01008(4pp) (2014)

ЖУРНАЛ НАНО- ТА ЕЛЕКТРОННОЇ ФІЗИКИ
Том **6** № 1, 01008(4cc) (2014)

Synthesis and Characterization of Nickel Ferrite: Role of Sintering Temperature on Structural Parameters

S.K. Emdadul Islam, Pankaj Sharma*

Department of Physics and Materials Science, Jaypee University of Information Technology, Waknaghat, Solan, H.P. (173234) India

(Received 30 October 2013; revised manuscript received 04 April 2014; published online 06 April 2014)

We synthesized Nanocrystalline nickel ferrite powder using co-precipitation method and studied the effect of sintering at 100, 400, 600, 800 °C on the prepared samples. X-ray diffraction (XRD) and transmission electron microscopy (TEM) were used to characterize the samples. XRD patterns show crystalline nature of the sample and the spinel structure of $NiFe_2O_4$. Particle size and morphology of the nanocrystalline powders were determined by TEM. The average particle sizes were identified to be 10 nm. Results indicate that the chemical synthesis by co-precipitation method leads to obtain nano crystalline nickel ferrite with controllable particle size.

Keywords: Co-precipitation, Ferrites, Structural parameters.

PACS numbers: 75.50.Gg, 73.63.Bd

1. INTRODUCTION

Magnetic nanopowders of spinel ferrites (MFe_2O_4, M = Ni, Co, Mn, Zn etc) are one of the important materials which was first synthesized about 50 years ago [1] and it has got high attention since few decades due to their useful electromagnetic characteristics for a huge number of technological applications such as information storage system, radio frequency coils, transformer, medical field for MRI, sensor, as radar absorbing materials (RAM) in military to increase the invisibility to radar etc [2-9]. This is mainly due to their properties are vastly differ from the corresponding bulk material. The function of these bulk ferrite materials is limited to a few megahertz frequency due to high electrical conductivity and domain wall resonance [10-11]. But in recent time's electronic industry demand more compact cores for work at higher frequency [12]. This problem of domain wall resonance could be avoided by synthesizing ferrite nanoparticles. In this case domain formation is not favorable energetically below a critical dimension of the particle and it exists as a single domain [13]. Ferrite nanoparticles can be synthesized by wet chemical method such as co-precipitation [14], sol-gel [15], reverse micelles [16], polymeric precursor and hydrothermal process [17-18]. The formula of the cubic structure of spinel ferrites are described as $[A][B]_2O_4$, where A is the tetrahedral and B is octahedral cation sites, in a FCC anion (oxygen) sublattice. $NiFe_2O_4$ has a normal spinel structure with Ni^{2+} ions in the A-site and Fe^{3+} ions in the B-sites [19].

In the present work, we have used the co-precipitation method due to its low cost, tailor made synthesis conditions and is very simple method to provide homogeneous powders in greater amount at temperature close to 60 °C [20]. Several preparation conditions such as concentration, molar ratio of the cation, pH of the solution and temperature can have an impact on the particle size of the ferrites and their properties [21]. $NiFe_2O_4$ powders are sintered at different temperatures. The lattice constant, crystal strain, dislocation density, phase of the ferrites and structural morphology of the nanocrystalline powders were studied.

2. EXPERIMENTAL DETAILS

2.1 Chemicals

Nickel chloride ($NiCI_2.6H_2O$); anhydrous ferric chloride ($FeCl_3$); Sodium Hydroxide (NaOH). All chemical were purchased from Merck (AR Grade) and used without further purification.

2.2 Synthesis

Nickel ferrite powders with compositions $NiFe_2O_4$ have been synthesized via co-precipitation method. Firstly, 0.5M $NiCl_2.6H_20$ solution is made by adding 11.88g in 100ml of double distilled water, simultaneously, 1M anhydrous $FeCl_3$ solution is made by adding 16.22 g in 100 ml of double distilled water. 0.4N NaOH solution (4 g NaOH pallet in 250 ml of distilled water) is used as precipitating agent. 50 ml of nickel chloride solution and 50 ml of ferric chloride solution were mixed and kept at 60 °C for 30 minutes. In this mixture, added the boiling NaOH solution under constant stirring till the pH of the solution becomes 12. Nanoferrites are formed by conversion of metal salts into hydroxides, followed by transformation of hydroxides into ferrites. The final solution was maintained at 85 °C for 80 minutes, this time is sufficient for the transformation of hydroxides into spinel ferrite. Particles were filtered from the solution and were washed several times with double distilled water. Collected particle were then dried at 80 °C. The samples were then grinded using mortar pestle and sintered at 100 °C, 400 °C, 600 °C and 800 °C for 4 hrs. The precipitated ferrite is chocolate brown in colour. The overall chemical reaction for the formation of $NiFe_2O_4$ may be written by the following way [22-23]:

$$Ni^{2+} + 2Fe^{3+} + 8OH^- \longrightarrow NiFe_2O_4 + 4H_2O$$

2.3 Characterization

The phase identification of the synthesized powder sample of $NiFe_2O_4$ was done by using X-ray diffractom-

* pks_phy@yahoo.co.in

eter (XRD) having Cu-Ka radiation. Goniometer = PW3050 / 60 (Theta / Theta); Minimum step size 2θ: 0.001; Minimum step size Omega: 0.001. The structural morphology is investigated using transmission electron microscopy (TEM)[Hitachi, H-7500, 40-120 kV operating voltage] at 90 kV.

3. RESULTS AND DISCUSSION

Fig. (1-4) shows the XRD patterns of powder samples after sintering at different temperatures 100 °C, 400 °C, 600 °C and 800 °C respectively. XRD data have been used to calculate structural parameters grain size, lattice parameter, strain of the crystal and dislocation density of the prepared sample. The average particle size of the sample was calculated by using Scherrer's formula [26]:

$$D = 0.9\lambda / \beta\cos\theta \quad (1)$$

where β is full width at half maxima and θ is Bragg's angle.

The average strain (ϵ) of the sample was calculated by Stokes Wilson equation [25]:

$$\epsilon = \beta/4\tan\theta \quad (2)$$

Equation is used to calculate the dislocation density [27],

$$\delta = 15\varepsilon / aD \quad (3)$$

where D is average grain size, a is lattice parameter[27]

$$a = d \times (h^2 + k^2 + l^2)^{0.5} \quad (4)$$

where d is spacing between two planes.

The values of parameters mentioned above are shown in Table 1. With increasing sintering temperature up to 600 °C crystal strain and dislocation density decreases due to an increase in particle size, but at 800 °C these parameters increases and particle size decreases. These changes in grain size, crystal strain and dislocation density may be due to the crystal deformation after certain temperature. Lattice parameter of the prepared sample decreases with increasing sintering temperature this is may be due to compactness of the lattice in the crystal increases.

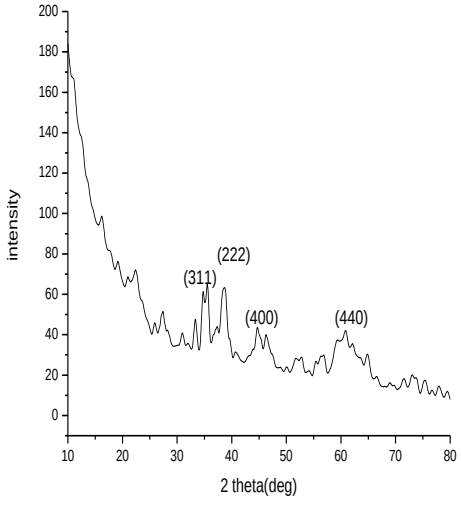

Fig. 1 – XRD Pattern for $NiFe_2O_4$ at a sintering temperature of 100 °C

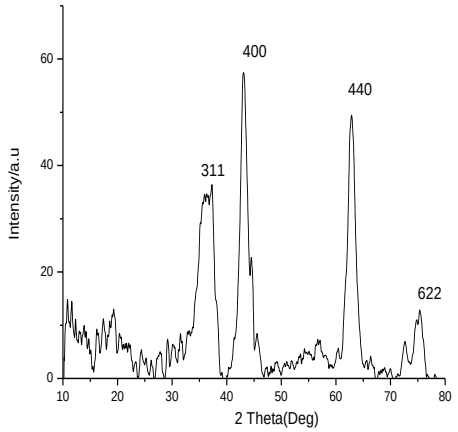

Fig. 2 – XRD Pattern for $NiFe_2O_4$ at a sintering temperature of 400 °C

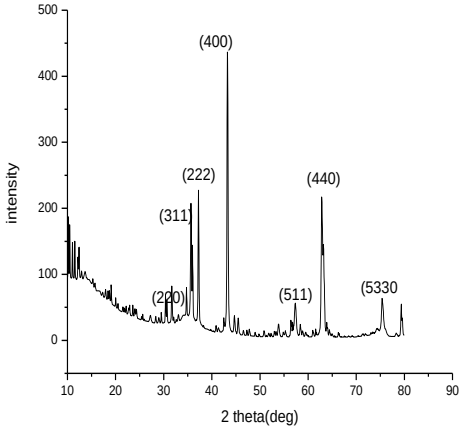

Fig. 3 – XRD Pattern for $NiFe_2O_4$ at a sintering temperature of 600 °C

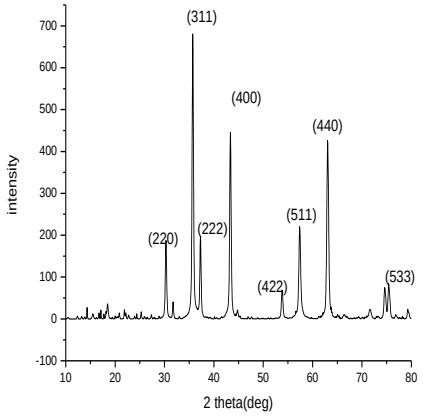

Fig. 4 – XRD Pattern for $NiFe_2O_4$ at a sintering temperature of 800 °C

The characteristic peaks of $NiFe_2O_4$ from figure 1-4 confirm the spinel structure of the powder sample and changes phase at different sintering temperature. The reflection peaks for 100 °C are corresponding to (311), (222), (400), (440) planes, for 400 °C the planes are (311), (400), (440) and (622) and for 600 °C and 800 °C planes are (220), (311), (222), (400), (511), (440) and (533) [24]. At 100 °C all the characteristic peaks are not intense, two broad lightly intense peaks for (311) and (222) plane are observed. Peak corresponding to (400)

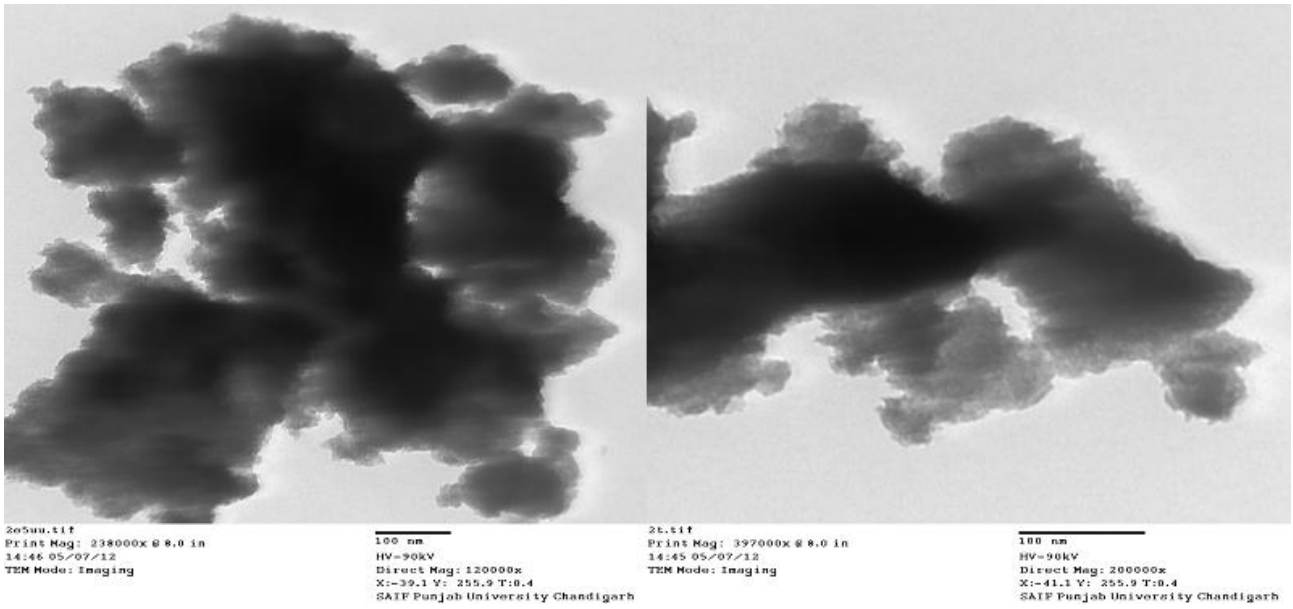

Fig. 5 – TEM Images for $NiFe_2O_4$ at a sintering temperature of 100 °C

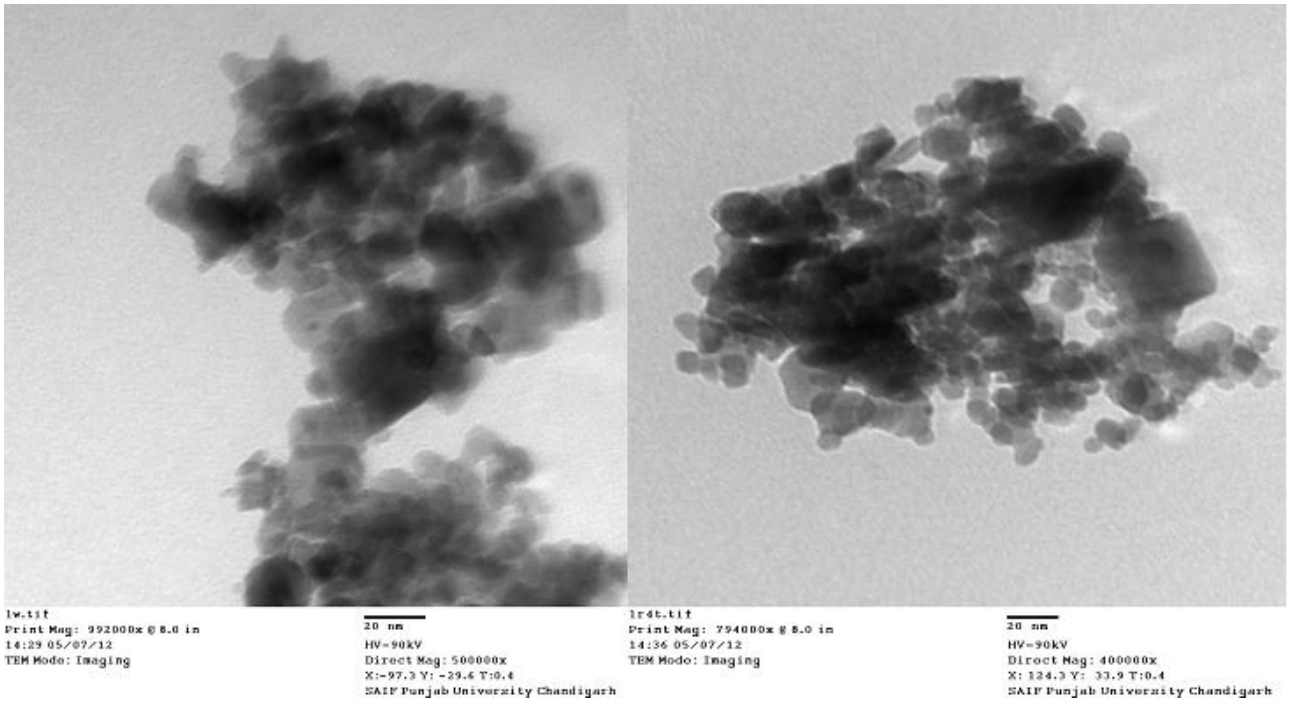

Fig. 6 – TEM Images for $NiFe_2O_4$ at a sintering temperature of 800 °C

Table 1 – Lattice Parameter, Strain and Dislocation Density for $NiFe_2O_4$ at a sintering temperature of 100, 400, 600 and 800 °C

Sintering Temperature (°C)	Lattice parameter (a) (Å)	Crystal Strain (ϵ)	Dislocation Density (δ)	Particle size (D) (nm)
100	8.3857	6.60×10^{-4}	4.5×10^{14}	26
400	8.3354	5.68×10^{-4}	2.7×10^{14}	37
600	8.3540	5.18×10^{-4}	2.3×10^{14}	42
800	8.3253	8.28×10^{-4}	5.3×10^{14}	28

plane is more intense for sintering temperature 400 °C in comparison to 100 °C. For sintering temperature 600 °C, sharp and more intense peaks are obtained for (400) plane along with (220), (511), and (533) planes. Comparing figures (1-4) all peaks become more intense and sharp with increasing sintering temperature *i.e.*, crystalline nature is increased. Since plane (400) has same intensity for sintering temperature 400 °C and 600 °C so confirms that the phase of the powder crystal is same. But ≥ 600 °C highly intense characteristic peaks

for (311) plane is found. It shows that phase changes above 600 °C sintering temperature and also with increasing the sintering temperature leads to higher crystallinity.

The TEM micrographs for $NiFe_2O_4$ powder are shown in fig. (5-6). The morphology of the prepared sample is mostly cubical with some agglomeration. The average particle size is estimated to about 10 nm for powder sintered at temperatures 100, 400, 600 and 800 °C for 4 hrs. The TEM micrograph of the powder sample at 100 °C in fig. (5) is not clear. It shows cloudy appearance supporting the XRD pattern of the sample with no intense peak. This may be due to the presence of moisture / impurities in the sample for 100 °C. But the micrograph images at 600 °C shown in fig. (6) are clear and are having cubical structure which is supporting our XRD results.

4. CONCLUSIONS

Nano-sized nickel ferrite particles were successfully prepared by co-precipitation method without any capping agent. Physically, the color of the precipitated powder changes from chocolate-brown to dark-brown and sometimes it becomes black when the sintering temperature is increased towards 800 °C.The average particle size is about 10 nm for powders sintered up to 800 °C. The observed results refer to change in phase of $NiFe_2O_4$ nanoparticles with increasing sintering temperature. XRD peak at different sintering temperatures show crystallinity of the prepared sample increasing with increasing the temperature. The cubical structure of the sample is confirmed by the TEM.

REFERENCES

1. Sh. Jabeli Moeen, M.R. Vaezi, A.A. Yousefi, *Prog. Color Colorants Coat.* **3**, 9 (2010).
2. C. Caizer, M. Propovici, C. Savii, *Acta Mater.* **51**, 3607 (2003).
3. Y.I. Kim, D. Kim, C.S. Lee, *Physica B.* **337**, 42 (2003).
4. D.K. Kim, Y. Zhang, W. Voit, K.V. Rao, M. Muhammad, *J. Magn. Magn. Mater.* 225, 30 (2001).
5. X. Li, Q. Li, Zh. Xia, W. Yan, *J. Alloy. Compd.* **458**, 558 (2008).
6. U.R. Lima, M.C. Nasar, R.S. Nasar, M.C. Rezende, J.H. Araujo *J. Magn. Magn. Mater.* **320**, 1666 (2008).
7. R. Bueno, M.L. Gregori, M.C.S. Nobrega, *J. Magn. Magn. Mater.* **320**, 864 (2008).
8. D.R. Sharma, R. Mathur, S.R. Vadera, N. Kumar, T.R.N. Kutty, *J. Alloy. Compd.* **358**, 193 (2003).
9. C.F.M. Costa, A.M.D. Leite, H.S. Ferreira, R.H.G.A. Kiminami, S. Cava, L. Gama, *J. Eur. Ceram. Soc.* **28**, 2033 (2008).
10. S.A. Morrison, C.L. Cahill, E.E. Carpenter, S. Calvin, R. Swaminathan, M.E. McHenry, V.G. Harris, *J Appl Phys.* **95**, 6392 (2004).
11. J.M. Daniels, A. Rosencwaig, *Can. J. Phys.* **48**, 381 (1970).
12. D. Stoppels, *J. Magn. Magn. Mater.* **160**, 323 (1996)
13. P.B.C. Rao, S.P. Setty, *Int. J. Eng. Sci. Tech.* **2(8)**, 3351 (2010).
14. M.U. Islama, T. Abbas, S.B. Niazi, Z. Ahmed, *Solid State Commun.* **130**, 353 (2004).
15. S. Zahi, M. Hashim, A.R. Daud, *J. Magn. Magn. Mater.* **308**, 177 (2007).
16. A.M. Shannon, L.C. Christopher, E.E. Carpenter, S. Calvin, V.G. Harris, *J. Appl. Phys.* **95,** 6392 (2004).
17. C.S. Kim, Y.S. Yi, K.-T. Park, H. Namgung, J.G. Lee, *J. Appl. Phys.* **85**, 5223 (1999)
18. A.K. Shrivastava, M.J. Hurben, M.A. Wittenauer, P. Kabos, C.E. Patton, R. Rameh, P.C. Dorsey, D.B. Chrisey, *J. Appl. Phys.* **85**, 7838 (1999).
19. L.D. Tung, V. Kolesnichenko, G. Caruntu, D. Caruntu, Y. Remond, V.O. Golub, C.J. O'Connor, L. Spinu, *Physica B* **319**, 116 (2002).
20. P.B.C. Rao, S.P. Setty, *Int. J Eng. Sc. Tech.* **2(8)**, 3351 (2010).
21. S. Khorrami, F. Gharib, G. Mahmoudzadeh, S. Sadat Sepehr, S. Sadat Madani, N. Naderfar, S. Manie, *Int. J. Nano. Dim,* **1(3)**, 221 (2011).
22. R.M. Cornell, U. Schertmann, *Iron Oxides in the Laboratory: Preparation and Characterisation* (Weinheim: VCH: 1999).
23. F.A. Cotton, G. Wilkinson, *Advanced inorganic chemistry* (New York: Wiley Interscience: 1988).
24. P.J. Binu, A. Kumar, R.P. Pant, S. Singh, E.M. Mohammed, *Bull. Mater. Sci.* **34(7)**, 1345 (2011).
25. M.G. Naseri, E.B. Saion, H.A. Ahangar, A.H. Shaari, M. Hashim, *J. Nanomater.* **2010**, 907686 (2010).
26. S. Kumar, P. Sharma, V. Sharma, *J. Appl. Phys.* **111**, 113510 (2012).
27. S. Kumar, P. Sharma, V. Sharma, *J. Appl. Phys.* **111**, 043519 (2012).